

INVESTIGATION OF LONGITUDINAL CRITICAL CURRENTS IN SUPERCONDUCTING
ALLOYS BASED ON Ti AND Zr

V. R. KARASIK and V. G. VERESHCHAGIN

P. N. Lebedev Physics Institute, USSR Academy of Sciences

Submitted December 26, 1969

Zh. Eksp. Teor. Fiz. 59, 36–47 (July, 1970)

Longitudinal critical currents ($j_c \parallel H$) in wire and ribbon samples prepared from the alloys Ti–22 at.% Nb, Zr–20 at.% Nb, and 65 BT are investigated. It is found that the maximum current is not determined by the nature of the structural defects but by the parameter H_c/λ . A study is made of the anisotropy of the critical current with respect to the angle between the wire axis and the external magnetic field for various mechanisms of destruction of superconductivity by the current. A condition for obtaining the highest attainable currents in superconducting alloys is formulated.

IN the investigation of critical currents in superconducting alloys, one distinguishes between the longitudinal currents $j_{c\parallel}$, when the external magnetic field H and the current flowing along the axis of the cylindrical sample are parallel, and the transverse currents $j_{c\perp}$, when the external magnetic field is perpendicular to the current.

The overwhelming majority of published data concern $j_{c\perp}$. Longitudinal critical currents were investigated very little. There is only one report^[1] of measurements performed in the entire range of existence of volume superconductivity ($0 \leq H \leq H_{c2}$). In^[1] they observed for the first time an unusual behavior of $j_c(H)$ for longitudinal currents, viz., the current increased with increasing external magnetic field and passed through a clearly pronounced maximum. This result was obtained with cold-deformed wire samples made of the alloys NbZr, TaTi, and MoRe. A maximum of $j_{c\parallel}(H)$ was observed later also in an investigation of ribbons coated with Nb₃Sn^[2].

Sekula, Boom, and Bergeron^[1] proposed that in a longitudinal magnetic field there occurs a force-free flow of current, such that $j \parallel H$ at each point of the sample, and the volume density of the Lorentz forces $f = j \times H/c$ vanishes identically.

Bergeron^[3] carried out a quantitative calculation of the $j_{c\parallel}(H)$ curve. Using for j_c an expression that follows from the laminar model of the mixed state^[4]

$$j_c = \frac{H_c}{4\pi\lambda} \left[1 - \left(\frac{H}{H_c} \right)^2 \tanh \frac{d_s}{2\lambda} \right]^{1/2} \quad (1)$$

(where H_c is the thermodynamic magnetic field, λ is the depth of penetration of the weak magnetic field, and d_s is the thickness of the superconducting lamella) and the solution of the equations of forced-free flow

$$4\pi j = \alpha H, \quad j = \frac{c}{4\pi} \operatorname{rot} H, \quad \operatorname{div} H = 0 \quad (2)$$

(Eqs. (2) have an analytic solution only for the case $\alpha = \text{const}$), it was shown that the $j_{c\parallel}(H)$ curve has a maximum. The value of the current at the maximum and at zero ($H = 0$) is determined by the ratio R/λ , where R is the radius of the sample. However, in the comparison of the theory^[3] with experiment^[1] it turned out that to

obtain satisfactory agreement it is necessary to admit of the existence of anomalously large values of λ .

Boyd^[5] calculated the longitudinal critical fields within the framework of the Ginzburg-Landau theory without any additional assumptions. He obtained the formula

$$\frac{4\pi j_c}{c} = \left(\frac{2}{3} \right)^{3/2} \frac{H_c(1 - H/H_{c2})^{3/2}}{\lambda\beta(1 - 1/2\kappa^2)}, \quad (3)$$

where β is a numerical factor of the order of unity and κ is a parameter of the Ginzburg-Landau theory.

Le Blanc^[6] advanced the hypothesis of helicoidal paramagnetic flow of current in a longitudinal magnetic field, as corroborated by measurements of the magnetization of the samples.

In^[7] they measured simultaneously the magnetization and the longitudinal current in alloys with an almost-reversible magnetization curve. It was shown that with increasing longitudinal current the magnetization decreases and vanishes when resistance appears in the sample. Formulas (1) and (3), and also the experimental results obtained in^[7], contain implicitly the general idea that the longitudinal critical currents are the limiting currents. Their values correspond to the vanishing of the difference of the free energies between the superconducting state in a given magnetic field and the normal state. But if this is so, then the value of $j_{c\parallel}$ should be determined by the ratio H_c/λ .

A verification of this assumption is the subject of the present paper. We incidentally investigated the dependence of the critical currents of wire samples on the angle between the axis of the wire and the external magnetic field. We also estimated numerically the values of the limiting currents. The results are compared with the experimental data.

1. MEASUREMENT PROCEDURE

The measurements were made on wire samples of 70–300 μ diameter prepared of alloys of titanium with niobium and zirconium with niobium. The procedure of preparing the samples is described in^[8], and their heat treatment and composition are indicated in the captions to the figures. The source of the magnetic field was a

superconducting solenoid having an inside-channel diameter 18 mm and a length 176 mm. The maximum field at the center of the working channel was 62 kOe. The samples were secured in removable holders which were alternately introduced into the solenoid channel during the course of the experiment. The first was used to measure the anisotropy of the critical currents, the second to investigate the longitudinal currents. The main elements of the holder are bulky copper current contacts, having a cross section in the form of a trapezoid, the large base of which is 13.5 mm, the small base 9 mm, the height 5 mm. The length of each contact was 38 mm; a brass shunt 3 mm long joined the current contacts. The shunt was soldered to the current contacts by silver solder. The resistance of the shunt at 4.2°K was 2×10^{-6} ohms. Potential contacts were soldered to the shunt. The current flowed from the holder plug to the current contacts through two flat copper leads with cross sections 8×1 mm, soldered to the current contacts with silver solder. The first holder was equipped with a grid of 0.5 mm mesh. In the holes were inserted pins that make it possible to set the working part of the sample at a given angle α to the direction of the external magnetic field. To monitor the accuracy of the sample setting, longitudinal lines were ruled on the second holder.

The investigated samples were soldered with indium, using an ultrasonic soldering device of the UZP-0.025 type with current contacts over the entire length. The true resistance in the current contacts in a 50 kOe magnetic field did not exceed 2×10^{-8} ohms at a current density in the samples 10^5 – 10^6 A/cm². The homogeneity of the magnetic field in the central part of the solenoid was not worse than 1% over a length of 50 mm. The accuracy with which the samples were set relative to the axis of the holder and their diameter were determined with the aid of a measuring microscope. The critical current was determined from the jump of the voltage across the shunt, as determined by an F-116 microvoltmeter.

The described construction of the holder had made it possible to pass currents up to 500 A through thin wire samples.

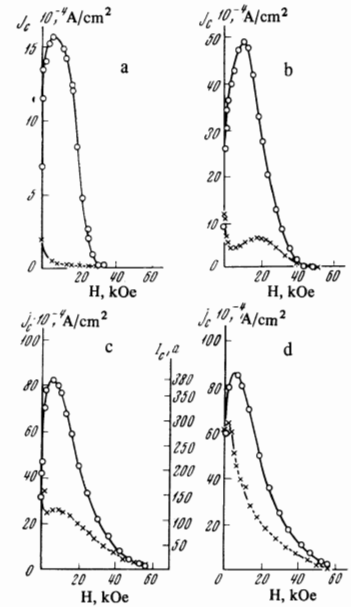
2. LONGITUDINAL CRITICAL CURRENTS

The most complete information concerning the nature of the destruction of superconductivity by current in a longitudinal magnetic field can be obtained by comparing the $j_{c\parallel}(H)$ and $j_{c\perp}(H)$ curves for samples with different structural states.

Figures 1a–1d show the $j_{c\parallel}(H)$ and $j_{c\perp}(H)$ curves obtained for recrystallized samples prepared of the alloy Ti–22 at.% Nb and subjected to different aging times at $t = 390^\circ\text{C}$. As is well known^[8], ω -phase particles that are uniformly distributed over the volume are separated in this alloy during the course of aging. The particles have the form of ellipsoids of revolution and increase in size during the aging process. Simultaneously, they become poorer in niobium. The equilibrium composition of the ω phase (~ 12 at.% Nb) is established at $t = 390^\circ\text{C}$ after 10 hours.

From the data of dark-field electron transmission microscopy using micro diffraction, obtained by Buřnov

FIG. 1. Alloy Ti–22 at.% Nb. Longitudinal (O) and transverse (X) critical currents of samples recrystallized at $t = 800^\circ\text{C}$ and subjected to different aging times at $t = 390^\circ\text{C}$: a—sample 1, diameter 245 μ , recrystallization time 1 hr; b—sample 2, diameter 249 μ , aging time 1.5 hr; c—sample 3, diameter 237 μ , aging time 3 hr; d—sample 4, diameter 230 μ , aging time 10 hr.



and Vazilkin^[9], at an aging temperature 390°C the ω ellipsoids have the following dimensions:

Aging time, hr	Axis dimensions, Å
1	250 × 90
10	440 × 160

From an analysis of Fig. 1 we see that, in full agreement with^[8], the behavior of the transverse currents is determined by the relation between the dimensions of the core of the Abrikosov vortex ($\xi \sim 100$ Å) and the dimensions of the ω ellipsoids. In recrystallized samples, the transverse critical currents are very small, since the vortex lattice is maintained only by the “background”—the residual dislocations, grain boundaries, and randomly distributed inhomogeneities (Fig. 1a). When the dimension of the ω particles becomes comparable with ξ , a maximum connected with the breakdown of the superconductivity in the ω particles appears on the curves. With increasing particle size and with approach of their composition to equilibrium, the maximum shifts towards weaker fields (Fig. 1b, c) and then vanishes (Fig. 1d).

The $j_{c\perp}(H)$ curves shown in Fig. 1 have different shapes, thus indicating the action of different mechanisms of superconductivity destruction by the current. In sample 1, at all values of the external magnetic field, and in samples 2 and 3 up to the maximum on the $j_{c\perp}(H)$ curve, the superconductivity is destroyed under the influence of the Lorentz force (the Kim-Anderson mechanism^[10]). In the region of fields beyond the maximum, and in sample 4 at all values of the field, the transition to the normal state is connected with the attainment of the critical velocity of the superconducting condensate^[8].

A different picture is observed in the analysis of the longitudinal-current curves plotted for the same samples. For convenience in the analysis, these curves are drawn in Fig. 2 in the same scale. It is seen (Fig. 2) that in all four samples j_c increases with increasing H , passes through a maximum, and then decreases rapidly as H_{c2} is approached. At the same time, the absolute values of the initial current and of the heights of the maxima of $j_{c\parallel}(H)$, and H_{c2} are different.

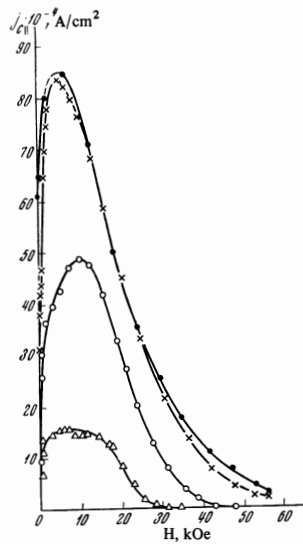


FIG. 2

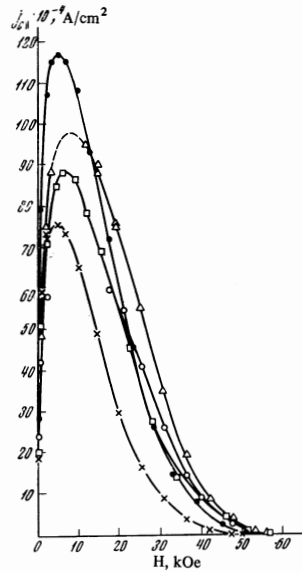


FIG. 3

FIG. 2. $j_{c\parallel}(H)$ curves of samples 1 (Δ), 2 (O), 3 (X), and 4 (\bullet), plotted in the same scale.

FIG. 3. Longitudinal critical currents of cold-deformed samples, prepared from the alloy Ti-22 at.% Nb: O —sample 8, degree of cold deformation $\beta = d_0^2/d^2 = 15.4$, diameter 304μ ; Δ —sample 9, $\beta = 82.6$, diameter 226μ ; \square —sample 10, $\beta = 651.9$, diameter 236μ ; X —sample 11, $\beta = 3044$, diameter 142μ ; \bullet —sample 12, $\beta = 5289$, diameter 111μ .

The fact that the $j_{c\parallel}(H)$ curves have all the same shape indicates that the same mechanism causes destruction of the superconductivity. When the directions of the transport current and of the external magnetic field coincide, the Lorentz force tends to zero, and only the perturbations act on the vortex lattice. The presence of perturbations is connected with the nonideal character of the force-free flow, due to the distortion of the structure of the sample, the inhomogeneity of the external magnetic field, the inaccurate setting of the sample, etc. Since the perturbations are small in magnitude, to stabilize the vortex lattice at $j \parallel H$ it suffices to have a small number of defects compared with the case of $j \perp H$.

It is practically impossible to produce a superconducting alloy containing no defects. The vortex lattice is therefore stabilized in the case of a longitudinal current, and the destruction of the superconductivity is connected with the attainment of the critical velocity by the condensate.

Analogous results were obtained with recrystallized samples 5, 6, and 7, prepared of the same alloy and subjected to aging of different duration at $t = 425^\circ\text{C}$.

Samples 5, 6, and 7 contain ω ellipsoids with the following dimensions^[9]:

Sample number	Aging time, hr.	Axis dimensions, \AA
5	1	300×120
6	3	450×160
7	10	900×380

Just as in the preceding series, the shape of the $j_{c\perp}(H)$ curves of samples 5, 6, and 7 are different. In sample 5 one observes a "peak effect"^[1] ($d \sim \xi(T)$),

¹⁾ d —dimension of the minor semi-axis of the ellipsoid.

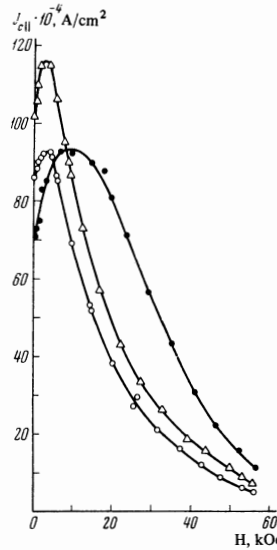


FIG. 4

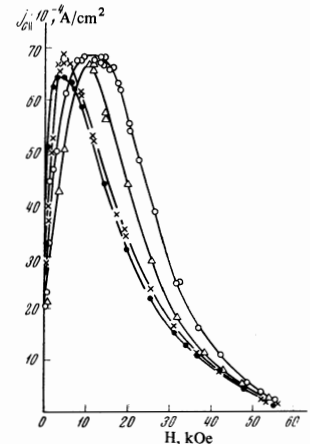


FIG. 5

FIG. 4. Longitudinal critical currents in cold-deformed samples made of the alloy Ti-22 at.% Nb and subjected to subsequent aging for one hour at 425°C : \bullet —sample 13, $\beta = 635.5$, diameter 232μ ; O —sample 14, $\beta = 3044$, diameter 141μ ; Δ —sample 15, $\beta = 5289$, diameter 102μ .

FIG. 5. Longitudinal critical currents in samples made of an alloy of Zr-20 at.% Nb, recrystallized at $t = 800^\circ$ for one hour and subjected to subsequent aging of different duration at $t = 450^\circ\text{C}$: O —sample 16, diameter 421μ ; Δ —sample 17, diameter 246μ , aging time one hour; X —sample 18, diameter 236μ , aging time 3 hours; \bullet —sample 19, diameter 241μ , aging time 5 hours.

while for samples 6 and 7 the vortex lattice is rigidly stabilized ($d > \xi(T)$). At the same time, the longitudinal-current curves are similar in form.

Figure 3 shows the $j_{c\parallel}(H)$ plots obtained for samples of the alloy Ti-22 at.% Nb, subjected to different degrees of cold deformation. The deformation stimulates the decay of the solid solution with segregation of finely-dispersed particles of the α phase with spindle-like shape^[8]. An investigation of the transverse currents has shown that, as a result, the vortex lattice becomes rigid even at small degrees of cold deformation^[8]. It follows from Fig. 3 that, just as in the preceding cases, the $j_{c\parallel}(H)$ curves have a characteristic dome-like shape. Just as for the transverse current^[8], no regular connection between the position of the curves on the diagram and the degree of cold deformation was observed for the $j_{c\parallel}(H)$ curves obtained for samples 8-12. The absence of a regularity is apparently connected with the influence of the different random factors on the rate of decay of the solid solution under the influence of plastic deformation (heating upon deformation, heat transfer, etc.).

We note, however, that a connection exists between the position of the maximum on the $j_{c\parallel}(H)$ curves and the mechanism of destruction of the superconductivity by current in a transverse field. Let us consider this connection, using as an example samples 13, 14, and 15, subjected to cold deformation and subsequent aging during one hour at $t = 425^\circ\text{C}$ (Fig. 4). According to the measurements of $j_{c\perp}(H)$, the superconductivity of sample 13 is destroyed in a transverse field under the influ-

ence of a Lorentz force, whereas for samples 14 and 15, in accordance with the same data, the superconducting condensate reaches the critical velocity in the entire region $H_{C1} < H < H_{C2}^{[8]}$. Accordingly, the maxima on the $j_{C\parallel}(H)$ curves of samples 14 and 15 occur in weak magnetic fields (5 kOe), while that of sample 13 is shifted towards stronger fields (see Fig. 4).

A similar regularity was observed for samples with different structural constants. At the same time, the $j_{C\parallel}(H)$ curves of samples 14 and 15 have different maxima, a fact that can be easily explained: in sample 15, which has a larger degree of prior cold deformation, the decay preceded deeper, the matrix was more enriched with niobium, H_C increased, and consequently the condensation energy and j_{\max} also increased.

In conclusion, let us consider the results obtained with other alloys.

Figure 5 shows the results of the measurement of $j_{C\parallel}(H)$ of recrystallized samples prepared of the alloy Zr-20 at.% Nb and subjected to aging of different duration at $t = 450^\circ\text{C}$. A characteristic feature of this alloy is the slight change of the superconducting properties of the matrix during the aging process when the matrix becomes enriched with niobium.

In this connection, the values of H_{C2} of samples 16, 17, 18 and 19 are the same. Using the alloy Zr-20 at.% Nb as an example, one can clearly see the independence of $j_{\parallel\max}$ of the character of the defects, of their dimension, and of their concentration. At the same time, with increasing duration of the aging, the position of the maximum shifts to the left. With the aid of the measurements of $j_{C\perp}(H)$ it was established that the motion of the maximum from right to left is connected with a transition from the Lorentz mechanism of destruction of superconductivity (sample 16) to a rigid vortical lattice (sample 19) and with the structure of the defects (see Sec. 5 below).

In order to estimate the influence of the geometry of the sample on the shape of the $j_{C\parallel}(H)$ curve, measurements were made on flat ribbons of the alloy Zr-20 at.% Nb, prepared by cold deformation, and on a recrystallized ribbon made of the alloy 65BT.

The $j_{C\parallel}(H)$ curves of the ribbon samples have the same characteristic domes as the curves of wire samples. However, the obtained current densities are lower, this being apparently connected with the distortion of the shape: the ribbons were deformed in two planes during the course of production, and it was impossible to set them exactly in the direction of the magnetic field.

3. CRITICAL-CURRENT ANISOTROPY OBSERVED UPON VARIATION OF THE ANGLE BETWEEN THE SAMPLE AXIS AND THE EXTERNAL MAGNETIC FIELD

The magnitude of the critical-current anisotropy depends strongly on the mechanism of destruction of the superconductivity in a transverse magnetic field. The largest anisotropy is observed if the superconductivity is destroyed under the action of the Lorentz force at $\alpha \neq 0$.

Figure 6 shows the results of measurements of $j_C(H)$ obtained with wire samples made by cold deformation

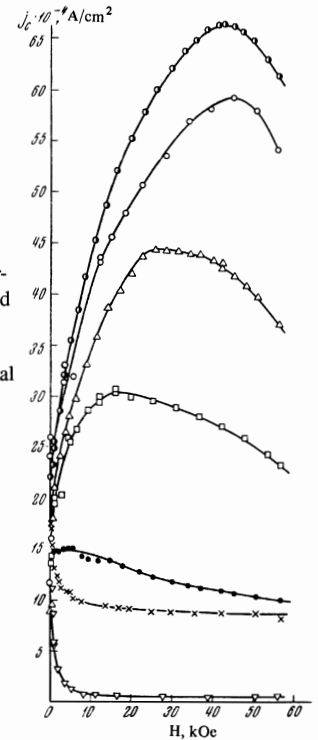


FIG. 6. Anisotropy of critical current in a wire sample prepared by cold deformation from the alloy Ti-36 at.% Nb, diameter 170μ ; α -angle between the sample axis and the external magnetic field: \bullet - $\alpha = 0^\circ$, \circ - $\alpha = 3^\circ$, Δ - $\alpha = 4^\circ$, \square - $\alpha = 6^\circ$, \bullet - $\alpha = 8^\circ$, \times - $\alpha = 9^\circ$, ∇ - $\alpha = 90^\circ$.

from the alloy Ti-36 at.% Nb. In this alloy, no decay takes place following cold deformation, and the main form of the defects are dislocations, capable of reliably stabilizing the vortex lattice only as $\alpha \rightarrow 0$, when the Lorentz force is small. The current decreases by a factor of 2, 7, and 110 at $\alpha = 6^\circ$, 9° , and 90° , respectively.

The smallest anisotropy of the critical current is observed in samples in which the rigid vortex lattice exists at all values of α and $H > H_{C1}$ ($0 \leq \alpha \leq 90^\circ$, $H_{C1} < H < H_{C2}$). Typical $j_{C\parallel}(H)$ and $j_{C\perp}(H)$ curves for a rigid vortex lattice, are shown in Fig. 1d. We see that in the case of a rigid lattice the longitudinal currents exceed the transverse ones by not more than a factor of 2. The same relation between $j_{C\parallel}$ and $j_{C\perp}$ was observed also for samples 6, 7, 15, and 19.

The incomplete isotropy of j_C in the presence of a rigid vortex lattice is apparently connected with two circumstances: (a) the difference between the current distributions over the cross section at $j_{\parallel H}$ and $j_{\perp H}$ and (b) the difference between the conditions of current flow along and across the Abrikosov vortices.

A case intermediate between strong and weak anisotropy is realized if a peak effect is observed in a transverse magnetic field. Ahead of the peak, the Lorentz mechanism of superconductivity destruction is effective, while past the peak the mechanism is that of destruction of electron pairs when critical velocity is reached.

Figure 7 shows data obtained for a recrystallized sample made of the alloy Ti-22 at.% Nb subjected to aging for one hour at $t = 390^\circ\text{C}$. We see that the peak effect is observed at all angles exceeding $3-4^\circ$. A slight inaccuracy in the setting of the sample is sufficient to distort the result: instead of a curve with a dome, characteristic of $j_{C\parallel}(H)$, a peak effect is observed²⁾.

²⁾Such an error was made in [11].



FIG. 7. Anisotropy of critical current in a recrystallized wire sample made of the alloy Ti-22 at.% Nb and subjected to the following aging for one hour at $t = 380^\circ\text{C}$, diameter 0.114 mm, \bullet — $\alpha = 90^\circ$, \times — $\alpha = 73^\circ$, \circ — $\alpha = 53^\circ$, Δ — $\alpha = 22.5^\circ$, \square — $\alpha = 10.5^\circ$, \bullet — $\alpha = 6^\circ$, ∇ — $\alpha = 0^\circ$.

In the region beyond the peak, as in all other cases where a rigid vortex lattice was observed, $j_{c\parallel}(H)$ exceeds $j_{c\perp}(H)$ by two times. Ahead of the peak, the maximum of the ratio is $j_{c\parallel}(H)/j_{c\perp}(H) \approx 6.5$.

4. DEPENDENCE OF THE CRITICAL CURRENT DENSITY ON THE SAMPLE DIAMETER

In order to explain the character of the distribution of the current over the cross section at different values of the external magnetic field, the longitudinal critical currents were plotted for samples of equal diameter (Fig. 8). In plotting the curves shown in Fig. 8, the total critical current I_c measured in the experiment was divided by the cross section area of the wire. We see that in an external magnetic field exceeding 20 kOe, the current density does not depend on the diameter; consequently, the current fills the cross section uniformly. In fields from 0 to 20 kOe, in the region of the dome, the average current density is the larger, the smaller the diameter of the sample, and the maximum on the $j_{c\parallel}(H)$ curve shifts to the right with increasing diameter. The results can be attributed to the filling of the cross section of the sample with current and to the influence of the magnetic field of the current. In a zero magnetic field, the current flows near the surface at an effective penetration depth λ^* . Therefore the quantity $f_c(0)$ is controlled by the parameter λ^*/R . The actual current density is $I_c/2\pi R\lambda^*$, and the current density averaged over the cross section is $I_c/\pi R^2$. Their ratio is proportional to λ^*/R and tends to saturation as $R \rightarrow \lambda^*$. Consequently, the maximum values of $j_c(0)$ were obtained with wires having a diameter on the order of λ^* .

The second consequence of the foregoing is the proportionality of the total currents in a zero field to the sample radii:

$$0.2I_1/R_1 = 0.2I_2/R_2 = H_{c1}^*, \quad (4)$$

where H_{c1}^* is the magnetic field of the current on the surface of the sample, at which the superconductivity is destroyed (the external field is equal to zero). In

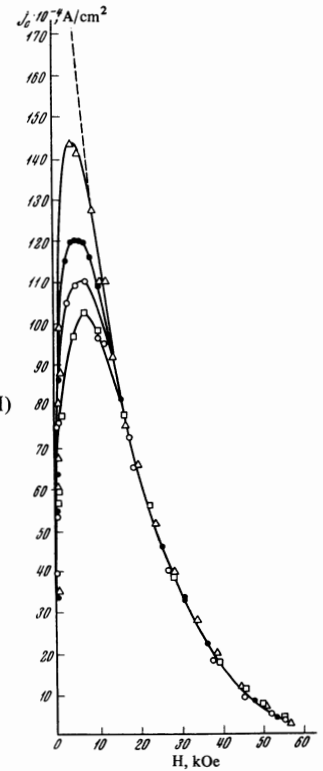


FIG. 8. Dependence of the form of the curve $j_c(H)$ on the sample diameter: Δ —diameter 0.090 μ ; \bullet —0.149 μ , \circ —0.205 μ , \square —0.233 μ , dashed curve—extrapolation for $f_{\mu c}(H) = 0$.

measurements made on the sample having a diameter of 233 μ , it was found that $I_c(0) = 62.6$ A, while for a sample with 90 μ diameter $I_c(0) = 23$ A. We see that relation (4) is satisfied with accuracy not worse than 4%.

With increasing external magnetic field H , the cross section of the sample begins to be filled with current. The total current increases, as does its magnetic field H_1 , which reaches a maximum value on the surface of the sample. According to Fig. 8, at the maximum $H_1 \approx H$: For a sample with 90 μ diameter, $H_1 = 4100$ Oe and $H \approx 4000$ Oe, whereas for a sample with 233 μ diameter $H_1 = 7500$ eV and $H \approx 8000$ Oe.

The current's own field is a serious limitation on the maximum current. For example, at a sample diameter 200 μ and a current density 10^7 A/cm² we have $H_1 \approx 63$ kOe. In the alloys investigated by us, the second critical field H_{c2} is the same order of magnitude. Therefore the limiting currents can be obtained only with thin samples; at $R = 1$ and $j_c \approx 10^7$ A/cm², the field is $H_1 \approx 630$ Oe. Extrapolating our experimental data, we can state that with further decrease of the sample diameter the peaks on the $j_{c\parallel}(H)$ curves will lie one on top of the other inside a cone made up of the ordinate axis and the dashed line in Fig. 8. The dashed line is the asymptotic of j_c when $R \rightarrow \lambda^*$.

5. DISCUSSION OF RESULTS

Using the obtained experimental results, let us analyze two questions—the shape of the $j_{c\parallel}(H)$ curve, and the limiting currents in superconducting alloys.

1) Shape of $j_{c\parallel}$ curve. All the obtained $j_{c\parallel}(H)$ curves (Figs. 1–8) have maxima, but these maxima occur at different magnetic fields and at different ratios of the current density at the maximum to the current density in a zero magnetic field. This is clearly seen from

Fig. 1: with decreasing breakdown field of the ω particles, the maximum on the $j_{c\parallel}(H)$ curve moves to the left, and the ratio of the current at the maximum to the current of zero decreases from 5 for sample 1 to 1.5 for sample 4. A similar behavior of the $j_{c\parallel}(H)$ plots is observed for samples 5, 6, and 7. If we denote the magnetic field at which $j_{c\parallel}(H)$ reaches a maximum by H_m , then the indicated regularities can be briefly formulated as follows: in the Ti-22 at.% Nb alloy, the values of H_m/H_{c2} and $j_{c\parallel}(H_m)/j_c(0)$ decrease with increase of the region in which the "rigid" vortex lattice exists^[8].

In alloys in which the solid solution does not decay following cold deformation, the maximum moves to the right with increasing degree of cold deformation. We assume that the quantities H_m/H_{c2} and $j_{c\parallel}(H_m)/j_c(0)$ are connected with the character of the defects influencing the formation of the "force-free" flow of current. Let us explain this with cold-deformed Ti-36 at.% Nb as an example. When the wire is rolled, the plastic deformation gives rise to an axially-symmetrical structure of alternating layers with different properties (hardness, dislocation density, electron mean free path, etc.), leading to modulation of the free energy in the radial directions. At $H > 0$, when the current begins to fill the cross section and vortex rings of magnetic flux are formed and tend to become compressed, powerful potential barriers appear in their path. Therefore the cross section is filled slowly, and the maximum of $j_{c\parallel}$ shifts towards larger magnetic fields.

In the region beyond the minimum, where the current density does not depend on the sample diameter, the average current density $\langle j_c \rangle$ and the microscopic current density j_μ coincide, and $\langle j_c \rangle$ can be compared with formulas derived from energy considerations, such as (1), (3), and (5) (see below). An analysis of the form of our experimental curves shows that when $H \rightarrow C_2$ there is satisfactory agreement with the expression^[8]

$$j_c(H) = \frac{H_c}{4\pi\lambda} \left(1 - \frac{H}{H_{c2}}\right)^2, \quad (5)$$

and in the region intermediate between H_m and $H \rightarrow H_{c2}$ the curves obey the law

$$j_c(H) = \frac{H_c}{4\pi\lambda} e^{-H/H_c}. \quad (6)$$

The results do not agree with formula (3). The conclusions drawn in^[3] on the basis of formulas (1) and (2), that the current at the points $H = 0$ and $H = H_m$ is proportional to the square of the radius of the sample, are likewise not confirmed.

2) Limiting currents in superconducting alloys.

Formulas (1), (3), and (5) for the critical currents of destruction of pairs of electrons have been derived under the assumption that the magnetic field of the current is negligibly small compared with the external

magnetic field. This assumption is not realized in practice, since there always exists a region, depending on the sample diameter, in which $H_I \geq H$. In this region, the distribution of the current over the cross section has a complicated form, and as was already stated, $\langle j_c \rangle$ is not equal to the microscopic density j_μ . It is also necessary to take into account the fact that in formulas of type (1) and (5) the function $f(H/H_{c2})$ is only roughly approximate. Therefore the most correct way of comparing the theoretical and experimental values of the longitudinal currents is as follows:

- the $j_{c\parallel}(H)$ curve is extrapolated from the region where $\langle j_c \rangle = j_\mu$ to $H = 0$ (see the dashed curve in Fig. 8);
- the obtained value is compared with that obtained by the formula (see^[13])

$$j_c = 0.54H_c / 4\pi\lambda, \quad (7)$$

where H_c and λ are calculated with the aid of the formulas, using the known experimental values of T_c , γ , and H_{c2} :

$$H_c = T_c \sqrt{2\pi\gamma} [1 - (T/T_c)^2], \quad (8)$$

$$\lambda = (\varphi_0 H_{c2} / 4\pi H_c^2)^{1/2}, \quad (9)$$

where γ is the coefficient of the linear term of the specific heat.

In our case the extrapolation to $H = 0$ is facilitated by the fact in a semilogarithmic scale the exponential (6) yields a straight line that intercepts the current axis at the value $j_c(0)$. In comparing the experimental results with the calculated ones it is necessary to determine the fraction of the sample cross section filled with non-superconducting ω particles.

We present below the data for samples 6 and 7. In the reduction of the dark-field pictures obtained with an electron microscope at a magnification of 70,000, it was established that the superconducting part of the cross section of sample 6 amounts to 19.4%, while that of sample 7 is 20.6%.

The results of the calculations and the measurements are summarized in the table.

We note that formula (7) has been derived for a thin sample ($R \ll \lambda$), but it is precisely with this formula that our experimental data must be compared, since the current uniformly filling the cross section is extrapolated to zero.

It is seen from the table that at $j \parallel H$ the currents in the alloys are actually the limiting ones. As to the transverse currents ($j \perp H$), they reach the limiting values only if the vortex lattice is rigidly secured; the conditions for rigidly securing the lattice are formulated in^[8]. In this case $j_{c\perp}$ is on the average half as large as $j_{c\parallel}$ at all values of the external magnetic field.

Thus, in order to determine beforehand which $j_{c\perp \max}$ will occur in the given substance if it becomes possible to secure rigidly the vortex lattice, it suffices to meas-

Sample	erg/cm ³ (°K) ² [4]	H _{c2} , Oe at 4.2°K	H _{c2} , Oe at 4.2°K	H _c , Oe at 4.2°K	T _c , °K	$\alpha = \frac{\lambda}{R}$	ξ , Å	$j_{c\parallel}(0)$, A/ cm ² , in accordance with formula (7) at 4.2°K	extrapolated to zero field, experiment
6	7.65	8 · 10 ⁴	1120	3570	7.5	57	63	1.27 · 10 ⁷	1.4 · 10 ⁷
7	7.65	7.7 · 10 ⁴	1125	3572	7.8	57	63	1.26 · 10 ⁷	1 · 10 ⁷

ure the longitudinal critical current and to take into account the fact that $j_{c\perp\max} \approx (1/2)j_{c\parallel\max}$.

The authors are grateful to B. M. Vul for interest in the work and for valuable remarks, to A. I. Rusinov and V. G. Ershov for useful discussions, to G. T. Nikitin, D. V. Pronkin, T. G. Rakhmanin, and G. A. Agapov for help with the experiments.

¹S. Sekula, R. W. Boom, and C. J. Bergeron, Appl. Phys. Lett. **2**, 102 (1962).

²G. W. Cullen, G. D. Cody, and J. P. McEvoy, Phys. Rev. **132**, 577 (1963).

³C. J. Bergeron, Appl. Phys. Lett. **3**, 63 (1964).

⁴B. B. Goodman, Rev. Mod. Phys. **36**, 12 (1964).

⁵R. G. Boyd, Phys. Rev. **145**, 256 (1966).

⁶M. A. R. Le Blanc, Phys. Rev. **143**, 220 (1966).

⁷H. London and D. G. Walmsley, Proc. of XI Intern. Conf. on Low. Temp. Phys. II, 1968, p. 879.

⁸Yu. F. Bychkov, V. G. Vereshchagin, V. R. Karasik, G. B. Kurganov, and V. A. Mal'tsev, Zh. Eksp. Teor. Fiz. **56**, 505 (1969) [Sov. Phys.-JETP **29**, 276 (1969)].

⁹V. R. Karasik, Yu. F. Bychkov, V. G. Vereshchagin, M. T. Zuev, G. B. Kurganov, V. A. Mal'tsev, V. A. Vazilkin, and N. N. Buinov, Abstracts of 8th Internat. Conf. of the Socialist Countries on the Physics and Technology of Low Temperatures, Dresden, 25-29 November 1969.

¹⁰P. W. Anderson, Phys. Rev. Lett. **9**, 309 (1962).

¹¹Yu. F. Bychkov, V. G. Vereshchagin, M. T. Zuev, V. R. Karasik, G. B. Kurganov, and V. A. Mal'tsev, ZhETF Pis. Red. **9**, 652 (1969) [JETP Lett. **9**, 404 (1969)].

¹²H. B. Furth, M. A. Levine, and R. W. Waniek, Rev. Sci. Instr. **28**, 949 (1957).

¹³V. P. Silin, Zh. Eksp. Teor. Fiz. **21**, 1330 (1951).

¹⁴E. M. Savitskiĭ, B. Ya. Sukharevskii, V. V. Baron, A. V. Aleshina, and M. I. Bychkova, Paper at 6th All-Union Conference on Superconducting Alloys and Compounds, Moscow, May 1969, Nauka, in press.

Translated by J. G. Adashko